Journal of Integrative Neuroscience

J. Integr. Neurosci. **2026**; 25(7): 53240
https://doi.org/10.31083/JIN53240

Original Research

Role of Succinate Accumulation in Prolonged Febrile Seizure-Induced Neuronal Injury and Epileptic Seizures in Sprague-Dawley Rats

Yi Yuan[1,†], Xiaoqian Wang[1,†], Hua Zhou[1], Yunrong Zhang[1], Xiangdong Wu[1], Shuping Yin[1], Beiqi Zhang[1], Qiaoyun Wang[1], Shuang Li[2], Hongliu Sun[1,*], Yan Zhan[3,*]

[1]School of Pharmaceutical Sciences, Shandong Medical and Pharmaceutical University, 264003 Yantai, Shandong, China
[2]Department of Pharmacy, Yantai Affiliated Hospital of Shandong Medical and Pharmaceutical University, 264100 Yantai, Shandong, China
[3]Department of Neurology, Yantai Affiliated Hospital of Shandong Medical and Pharmaceutical University, 264100 Yantai, Shandong, China
*Correspondence: sun_china6@163.com; sunhongliu@sdmpu.edu.cn (Hongliu Sun); zhanyan2004@sina.com; zhany2022@sdmpu.edu.cn (Yan Zhan)
[†]These authors contributed equally.
Academic Editor: Moo-Ho Won
Submitted: 23 April 2026 Revised: 8 June 2026 Accepted: 12 June 2026 Published: 27 July 2026

Abstract

Background: Though succinate accumulation is a vital contributor to overexcitation and reactive oxygen species (ROS) production, whether it contributes to febrile seizures (FS) is unclear. We sought to mechanistically explore the role of succinate in prolonged FS. **Methods:** Prolonged FS were induced by hyperthermic treatment in Sprague-Dawley pups. Inhibitors of succinate dehydrogenase (SDH), purine nucleotide cycle (PNC), and malate/aspartate shuttle (MAS) were administered, respectively. Succinate levels and oxidative stress damage were assessed, and epileptic seizures and learning and memory ability were assessed after hyperthermic treatment. **Results:** Succinate levels increased significantly, accompanied by oxidative stress injury, seizures, and learning and memory defects, following prolonged FS. Treatment with the SDH inhibitor reduced succinate levels, accompanied by reduced levels of oxidative stress injury, attenuated seizures, and learning and memory deficits. Treatment with inhibitors of MAS and PNC, respectively, played similar protective roles, accompanied by decreased succinate levels. **Conclusions:** Increased succinate levels promote prolonged FS-induced oxidative stress injury and epileptogenesis. Reducing succinate accumulation may be a potential method for prolonged FS treatment. Moreover, elevated succinate levels may result from the reverse catalysis of SDH-targeting fumarate, which was produced from PNC and MAS.

Keywords: febrile seizure; succinates; oxidative stress; neuronal injury; epileptogenesis

1. Introduction

Febrile seizures (FS) are the most common seizures in childhood [1], affecting 2–5% of children [2]. Long-term recurrent attacks can lead to neuronal damage and learning and memory dysfunction and have irreversible effects on children's brain development [3,4]. In clinical practice, 37.1% of sudden, unexplained deaths in children are closely related to FS [5]. Current therapeutic strategies aim to reduce the excessive excitability using anti-seizure drugs. However, anti-seizure drugs are ineffective in approximately 50% of children with seizures and may aggravate the neurological deficits caused by FS [6] and even disrupt pediatric brain development [7]. Therefore, it is necessary to explore the mechanisms underlying FS-induced neuronal damage to identify potential therapeutic targets.

Excessive excitation is a vital pathological feature of FS. The brain affected by FS undergoes a battery of neurotoxic events, such as a massive release of excitatory neurotransmitters (e.g., glutamate) and overactivation of N-methyl-D-aspartic acid (NMDA) receptors [8,9]. Succinate is a critical regulator of the tricarboxylic acid cycle and glutamate-gamma aminobutyric acid (GABA) shunt [10], and its accumulation can induce overexcitation of neurons and neonatal seizures [9]. NMDA receptor antagonists significantly attenuate succinate accumulation-induced overexcitation [11]. Moreover, our previous study verified that succinate accumulation is a vital initiating factor of neuronal overexcitation in kainic acid-induced epilepsy [12].

The increased reactive oxygen species (ROS) due to overexcitation is closely related to oxidative stress-induced neuronal damage in FS [13,14]. Excessive excitation-induced defects in mitochondrial function suppress mitochondrial electron transport and produce ROS, eventually resulting in oxidative stress injury [14,15,16]. In contrast, mitochondrial damage aggravates ROS generation [17]. Furthermore, ROS accumulation influences Ca^{2+} homeostasis and promotes the release of excitatory amino acids, further intensifying excitation [18,19].

Succinate accumulation is an important contributor to ROS production. Succinate initiates the momentous fumarate-malate-oxaloacetate pathway [20,21]. Succinate dehydrogenase (SDH), a critical metabolic enzyme, oxidizes succinate to fumarate and maintains mitochondrial

ROS homeostasis by generating and eliminating superoxides [22]. However, in multiple pathological processes, SDH may reversely catalyze fumarate via malate/aspartate shuttle (MAS) and the purine nucleotide cycle (PNC), causing succinate accumulation. Subsequently, SDH reoxidizes accumulated succinate and produces excessive mitochondrial ROS via the reverse electron flow of NADH dehydrogenase [10,23,24].

Considering the effects of succinate accumulation on ROS generation and the important contribution of ROS to overexcitation and oxidative stress damage, which are vital pathological changes of FS, we hypothesized that succinate accumulation-induced excessive ROS generation may participate in the neuronal injury induced by FS. Therefore, we investigated alterations in succinate levels and explored the possible roles of accumulated succinate in prolonged FS in rats.

2. Materials and Methods

2.1 Animals

Pregnant Sprague-Dawley rats were obtained from Pengyue Experimental Animal Center (Jinan, Shandong, China) and housed individually with ad libitum access to food and water. In accordance with ARRIVE 2.0 (**Supplementary Material-ARRIVE**), all experiments were conducted between 9:00 and 17:00, and every effort was made to minimize animal discomfort and reduce animal usage.

According to the experimental design (**Supplementary Fig. 1**), this study included four experimental sections. In the first section, littermates were randomly divided into the control group (39 rats) and the prolonged FS group (59 rats); in the second section, littermates were randomly divided into the dimethyl malonate (DM) + prolonged FS group and the saline + prolonged FS group (38 rats/group); in the same way, littermates were randomly treated with aminooxyacetic acid (AOA) or 5-aminoimidazole-4-carboxamide-1-β-D-ribofuranoside (AICAR), and the controls were treated with saline (34 rats/group). The investigator was blinded to the group allocation during the experiment. After the experiment, the rats were sacrificed by intraperitoneal injection of pentobarbital sodium (CAS: 57-33-0, Xiya Reagent, Chengdu, Sichuan, China) at a dose of 150 mg/kg.

2.2 Hyperthermia-Induced Prolonged FS

We used 15–18 g P9 pups [25]. Same-litter pups were randomly assigned to control or prolonged FS groups. Prolonged FS were established following exposure to hyperthermia [2,14]. We prepared a thermostatic heating device with a closed transparent window to facilitate observation. The normal body temperature of each pup before modeling was recorded, and pups in the prolonged FS group were put in a thermostatic device (44 ± 0.5 °C) [25]. In accordance with previous reports, once the first FS was evoked, the pups were removed, left at room temperature for 2 min [26], then placed back in the thermostatic apparatus. The second FS continued for 10 min, after which the pups were again removed for 2 min. The 3rd and 4th FS were performed similarly to the 2nd one. The pups with prolonged FS received four seizures, and the controls were placed in the unheated device at the same time. In our study, 316 pups were used, and 6 pups were excluded (3 pups had no seizures in 55 min and 3 pups died during serious seizures).

2.3 Pharmacological Manipulations

According to our previous studies [12,27], on the 9th day after birth (P9: the weight of the young rats was approximately 15–18 g), DM (1.15 g/mL, 0.03 mL/kg; CAS: 108-59-8; Sigma-Aldrich, St. Louis, MO, USA), a competitive inhibitor of SDH, was injected intraperitoneally 15 min before hyperthermia treatment (DM + prolonged FS group). Instead of DM, saline was injected into the saline + prolonged FS group. With the rat-specific fixation device, P9 young rats were fixed on the stereotactic apparatus (ZH0003, Zhenghua Biological Instrument Equipment Co., Huaibei, Anhui, China); AOA (3.125 μg/μL, 0.53 mL/kg; CAS: 645-88-5; J&W Pharmlab, Shanghai, China), a specific MAS blocker, was injected into the right lateral ventricle (anteroposterior, –0.46 mm; mediolateral, 0.81 mm; and dorsoventral, –1.26 mm) 30 min before hyperthermia in the AOA + prolonged FS group, and the control group was treated with saline. In the same way, a specific inhibitor of PNC, AICAR (0.15 μg/μL dissolved in saline, 0.53 mL/kg; CAS: 2627-69-2; Acros, Geel, Belgium), was injected into the right lateral ventricle 60 min before hyperthermia (AICAR + prolonged FS group), whereas the corresponding control group was given saline.

2.4 Electroencephalography (EEG)

We chose the two-month time point to explore the long-term sequelae induced by early febrile seizures. As in our previous reports [14], EEG was continuously recorded at 2 months after prolonged FS treatment using the PowerLab system (PL3508, AD Instruments, Bella Vista, NSW, Australia) through stainless steel electrodes (791500, A.M. Systems, Sequim, WA, USA) planted in the left cortex (anteroposterior, –3.2 mm; mediolateral, –3.0 mm; and dorsoventral, –1.8 mm). Frequency and power spectrum densities (PSDs) were analyzed. The standard definition of seizures is multimodal discharge >5 Hz, which is two times higher than the baseline for ≥3 s duration.

2.5 Succinate Detection

At three time points during hyperthermia treatment (10 min, 15 min, and the end of prolonged FS modeling), the pups (n = 5/group) were randomly selected and anesthetized (sodium pentobarbital, i.p., 50 mg/kg, Xiya Reagent), and the hippocampus and cortex were removed rapidly on ice for succinate colorimetric assessment

(MAK184, Sigma-Aldrich) using a microplate reader at 450 nm, as described in our previous reports (three technical replicates/sample) [12,14].

2.6 Learning and Memory Ability

The Morris water maze test was used to assess the learning and memory abilities of rats 2 months after prolonged FS. The test was divided into a positioning navigation experiment (days 1–4) and a space exploration experiment (day 5). The tested circular pool included four quadrants, and the platform was placed in one quadrant under the water level by 1 cm. In the navigation experiment, rats were allowed to swim for 60 s to find the platform. For the spatial exploration experiment, the platform was removed, the rat was placed in a circular pool for 60 s, and its swimming trajectory was recorded. The learning and memory abilities of rats were evaluated by latency to the platform, cumulative percentage of time in the opposite and target quadrants, and number of crossings into the target quadrant.

2.7 Immunohistochemistry

Rats (n = 4/group) were randomly selected and anesthetized (sodium pentobarbital, 50 mg/kg, Xiya Reagent) 24 h and 3 days after modeling FS. Saline was injected rapidly into the left ventricle, followed by 4% paraformaldehyde (CAS 30525-89-4, Guoyao Reagent, Shanghai, China). The brains were fixed in 4% paraformaldehyde for 24 h, and then cryoprotected with sucrose solution until they sank. After flash-freezing the brains in liquid nitrogen, 11 µm thick brain sections were prepared using a cryostat microtome (CM3050 S, Leica, Wetzlar, Germany). Immunofluorescence staining was done as previously described (three technical replicates/sample) [28]. The primary antibodies applied included mouse anti-translocase of outer mitochondrial membrane 20 (TOMM20, 1:100; ab56783; Abcam, Cambridge, UK) and rabbit anti-microtubule-associated protein 1 light chain 3 beta (LC3B, 1:100; ab48394; Abcam). The sections were then washed with PBS and incubated with secondary antibody dilution buffer containing a mixture of Cy3 (1:200; A0516; Beyotime, Shanghai, China) or fluorescein isothiocyanate (FITC, 1:200; abs20003; Absin Bioscience, Shanghai, China) for 1.5 h in darkness. The sections were rinsed with PBS and incubated using 4',6-diamidino-2-phenylindole (DAPI) staining solution (1:3000; C1005; Beyotime) in darkness for 15 min. Images were viewed using a fluorescence microscope (Model BX53, Olympus, Tokyo, Japan) and quantified using ImageJ V.1.37 software (National Institutes of Health, Bethesda, MD, USA).

2.8 Fluoro-Jade B (FJB) Staining

FJB (AG310-30MG; EMD Millipore, Billerica, MA, USA) staining served to assess neuronal injury [29]. At 24 h, 3 days, and 2 months after modeling, 4 rats in each group were randomly selected to prepare 11 µm thick brain sections as aforementioned. Brain sections were sequentially soaked in 80% ethanol containing 1% NaOH for 5 min, 70% alcohol for 2 min, distilled water for 2 min, and 0.06% potassium permanganate solution for 15 min prior to distilled water rinsing. Subsequently, brain slices were immersed in 0.0004% FJB staining solution for 35 min and washed with distilled water. After drying, the brain slices were immersed in xylene for 2 min. Images were captured on a fluorescence microscope (Axio Imager 2, Carl Zeiss AG, Oberkochen, Germany) under 450 nm excitation light. Positive signals were counted (three technical replicates/sample).

2.9 Western Blotting

Four rats per group were randomly picked and anesthetized at 24 h, 3 days, and 2 months after modeling. The hippocampus and cortex were separated on ice, and proteins were extracted. Following protein quantification, different proteins were resolved on a 12% sodium dodecyl sulfate polyacrylamide gel (P0012A; Beyotime, China) before transfer onto polyvinylidene difluoride (PVDF) membrane (0.22 µm, Millipore). The membrane was blocked with 5% skim milk for 2 h, rinsed with tris-buffered saline with tween 20 (TBST, pH 7.4; CAS 9005-64-5, MeilunBio, Dalian, Liaoning, China), and incubated with primary antibodies at 4 °C overnight. The primary antibodies used were rabbit monoclonal LC3B (1:2000; ab48394, Abcam), caspase-3 (1:1000, 9662, Cell Signaling Technology, Danvers, MA, USA), activated caspase-3 (1:1000, ab2302, Abcam), and glyceraldehyde 3-phosphate dehydrogenase (GAPDH; 1:3000; AB-P-R001, Kangcheng, Shanghai, China). After washing with TBST, the membrane was incubated with horseradish peroxidase-conjugated IgG (goat anti-rabbit, SAB48169, Bio-swamp Biotechnology, Wuhan, Hubei, China) for 1.5 h at room temperature, then shaken in TBST on a shaker oscillator (CS-200, Youning, Hangzhou, Zhejiang, China). The PVDF membrane was visualized via an Odyssey Fc imaging system (LI-COR Bioscience, Lincoln, NE, USA) with a developer solution. Grayscale analysis of the target protein bands was performed using ImageJ software (National Institutes of Health, version 1.37), and the final result was the ratio of the target protein intensity to that of GAPDH (three technical replicates/sample).

2.10 ROS Estimation via DCF-DA

Four rats per group were randomly selected and anesthetized at 24 h post-modeling. The hippocampus and cortex were isolated on ice and placed in 0.01 M PBS. The tissue was crushed and filtered with a 200-mesh filter. 2',7'-dichlorodihydrofluorescein diacetate (10 mM, DCF-DA, S0033, Beyotime) was added to the filtrate [30]. After incubation at 37 °C for 30 min away from light, the tissue precipitate was centrifuged and washed for three times, and then detected with a Fluoroskan FL fluorescence and lu-

minescence microplate reader (Thermo Fisher Scientific, Waltham, MA, USA) at excitation and emission wavelengths of 470 nm and 525 nm, respectively (three technical replicates/sample).

2.11 Statistical Analyses

Data were expressed as mean ± SEM and processed via SPSS software (version 25.0; IBM, Armonk, NY, USA). Sample numbers were determined by a pre-experiment using balanced one-way analysis of variance (ANOVA). The data met normal distribution and variance homogeneity. Platform latency in the Morris water maze test was analyzed using two-way ANOVA. Categorical analysis among three or more groups was performed using one-way ANOVA; post-hoc multiple comparisons were conducted using the Tukey's method. Comparisons between two groups were performed using an unpaired *t*-test. The significance threshold was defined as $p < 0.05$.

3. Results

3.1 Elevated Levels of Succinate, Mitophagy and Oxidative Stress Injury After Prolonged FS

Succinate and DCF levels were measured in the control and prolonged FS groups. Succinate levels in the prolonged FS rats were significantly elevated (cortex, $p < 0.001$; hippocampus, $p < 0.001$; Fig. 1A), with increased levels of DCF in pups treated with prolonged FS (Fig. 1B). LC3B is an autophagy-associated protein [31]. Western blotting results indicated increased LC3B levels in prolonged FS pups (Fig. 1C,D, the original Western blotting images are provided in the **Supplementary Material-WB**). Immunofluorescence results indicated increased colocalization of TOMM20 and LC3B in the cortex and hippocampus (Fig. 1E–G) after prolonged FS. Most of the overlapping signals of LC3B and TOMM20 indicated that autophagy mainly occurred in the mitochondria.

Apoptosis and neuronal injury were also evaluated after prolonged FS. Western blotting results showed that activated caspase-3 levels after prolonged FS treatment were significantly increased (Fig. 1H,I), and caspase-3 levels were reduced (Fig. 1H,J, the original Western blotting images are provided in the **Supplementary Material-WB**). Neuronal injury was assessed by FJB staining, the results confirmed increased FJB positive signals in the cortex and hippocampus (Fig. 1K–M).

3.2 Epileptic Seizures and Weakened Learning and Memory Abilities After Prolonged FS

EEG was performed to evaluate epileptic seizures 2 months after prolonged FS. The frequency and cumulative time of epileptic seizures in males and females were analyzed after prolonged FS, and no differences were found between them (Fig. 2C,D). Representative EEG and PSD analyses are presented in Fig. 2A,B.

Moreover, the results of the Morris water maze test indicated the extended platform latency (female, $p = 0.02$; male, $p = 0.024$; Fig. 2E,F), with reduced target quadrant frequency (Fig. 2G), target quadrant time (Fig. 2I), and prolonged opposite quadrant time (Fig. 2H). These results verified the defective learning and memory abilities of rats with prolonged FS. A representative trajectory is shown in Fig. 2J. No significant differences were observed between females and males.

3.3 DM Treatment Decreased Succinate Levels, Mitophagy, Oxidative Stress Injury

DM is a competitive inhibitor of SDH [12]. We found that after the DM intervention, the levels of succinate (Fig. 3A) and DCF (Fig. 3B) in the DM + prolonged FS group were significantly reduced. Western blotting detection indicated reduced LC3B levels (Fig. 3C,D, the original Western blotting images are provided in the **Supplementary Material-WB**) in the DM + prolonged FS group. Immunofluorescence staining confirmed a decrease in LC3B (Fig. 3E,F) and TOMM20 levels (Fig. 3E,G) after DM treatment.

Moreover, reduced activated caspase-3 levels (Fig. 3H,I, the original Western blotting images are provided in the **Supplementary Material-WB**) and increased caspase-3 (Fig. 3H,J) were found in DM-treated rats, with decreased FJB signals in brain (Fig. 3K–M). These results indicated attenuated apoptosis and neuronal injury due to DM treatment.

3.4 DM Treatment Attenuated Seizures and Defective Learning and Memory Abilities in Prolonged FS-Treated Rats

The severity of seizures was assessed by EEG in rats 2 months after the DM intervention (Fig. 4A,B). The number (Fig. 4C) and cumulative time (Fig. 4D) of seizures in the DM + prolonged FS group significantly decreased. The water maze test results suggested that in DM + prolonged FS-treated rats, the prolonged platform latency induced by prolonged FS was reduced (Fig. 4E), with increased target zone frequency (Fig. 4F) and target quadrant time (Fig. 4G) and reduced opposite quadrant time (Fig. 4H). A representative trajectory is shown in Fig. 4I.

3.5 AOA Treatment Decreased Succinate Levels, Mitophagy, Oxidative Stress Injury

Administration of AOA, which is a specific inhibitor of MAS [12], led to decreased succinate (Fig. 5A) and DCF levels (Fig. 5B). Western blotting revealed reduced LC3B levels (Fig. 5C,D, the original Western blotting images are provided in the **Supplementary Material-WB**). Immunofluorescence results also confirmed the reduced TOMM20 and LC3B levels in the hippocampus and cortex (Fig. 5E–G) after AOA treatment.

Decreased activated caspase-3 levels and increased caspase-3 levels were found after AOA administration (Fig.

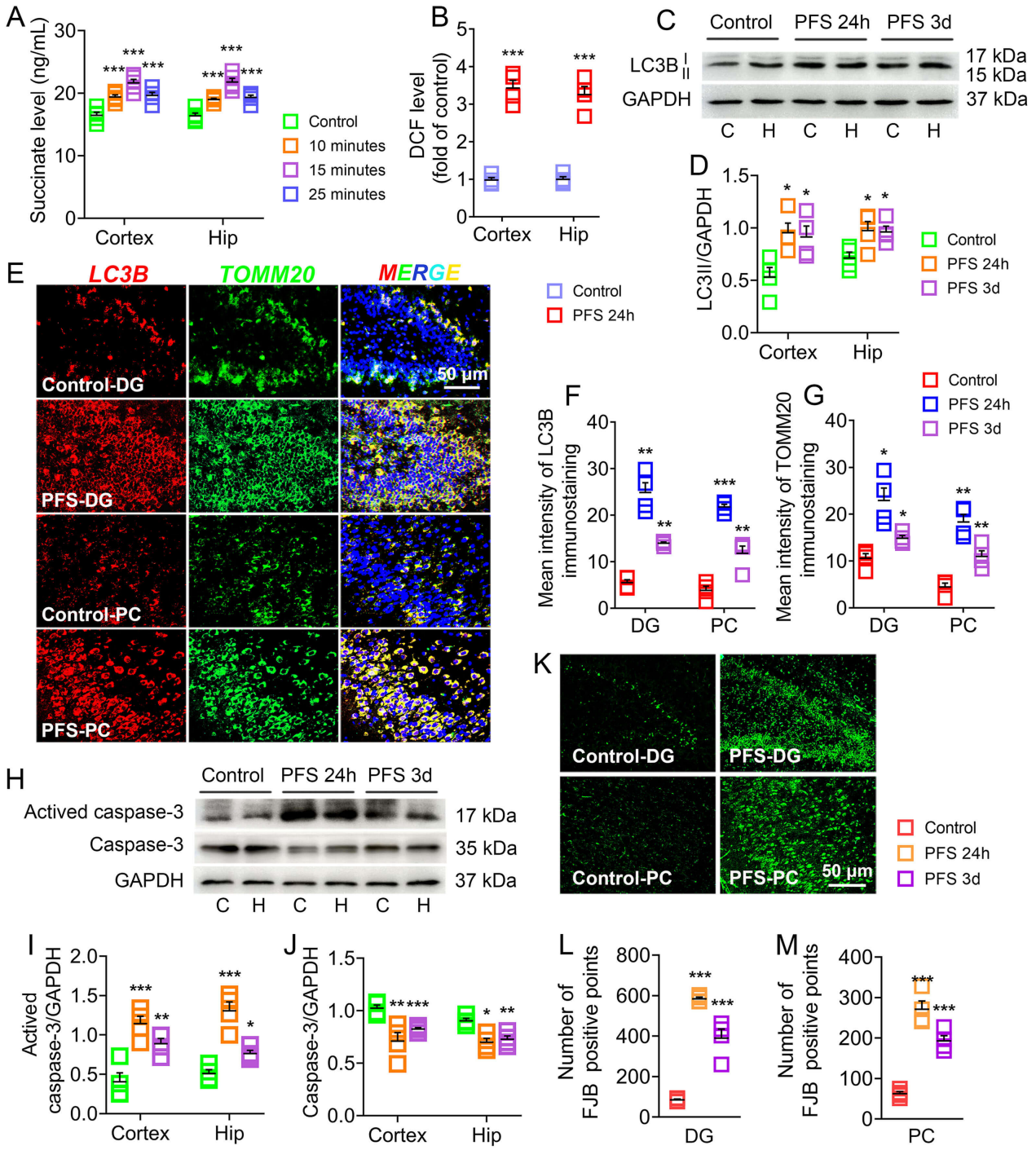

Fig. 1. Elevated levels of succinate, oxidative stress, mitophagy, and neuronal injury after prolonged FS. Elevated succinate (A) and DCF (B) in the hippocampus and cortex. (C,D) Gel bands and analysis of LC3B. Immunofluorescence images (E) and immunofluorescence analysis (F,G) of TOMM20 (green) and LC3B (red). DAPI, blue. Gel bands (H) and quantification results (I,J) of caspase-3 and activated caspase-3 (K–M) FJB staining results. Succinate detection, n = 5/group; the others, n = 4/group. *$p < 0.05$, **$p < 0.01$, ***$p < 0.001$, compared with the controls. DCF, 2',7'- dichlorodihydrofluorescein; GAPDH, glyceraldehyde 3-phosphate dehydrogenase; PFS, prolonged febrile seizures; DG, dentate gyrus; PC, piriform cortex; FJB, Fluoro-Jade B; FS, febrile seizures; DAPI, 4',6-diamidino-2-phenylindole; LC3B, microtubule-associated protein 1 light chain 3 beta; TOMM20, translocase of outer mitochondrial membrane 20. Scale bar = 50 μm.

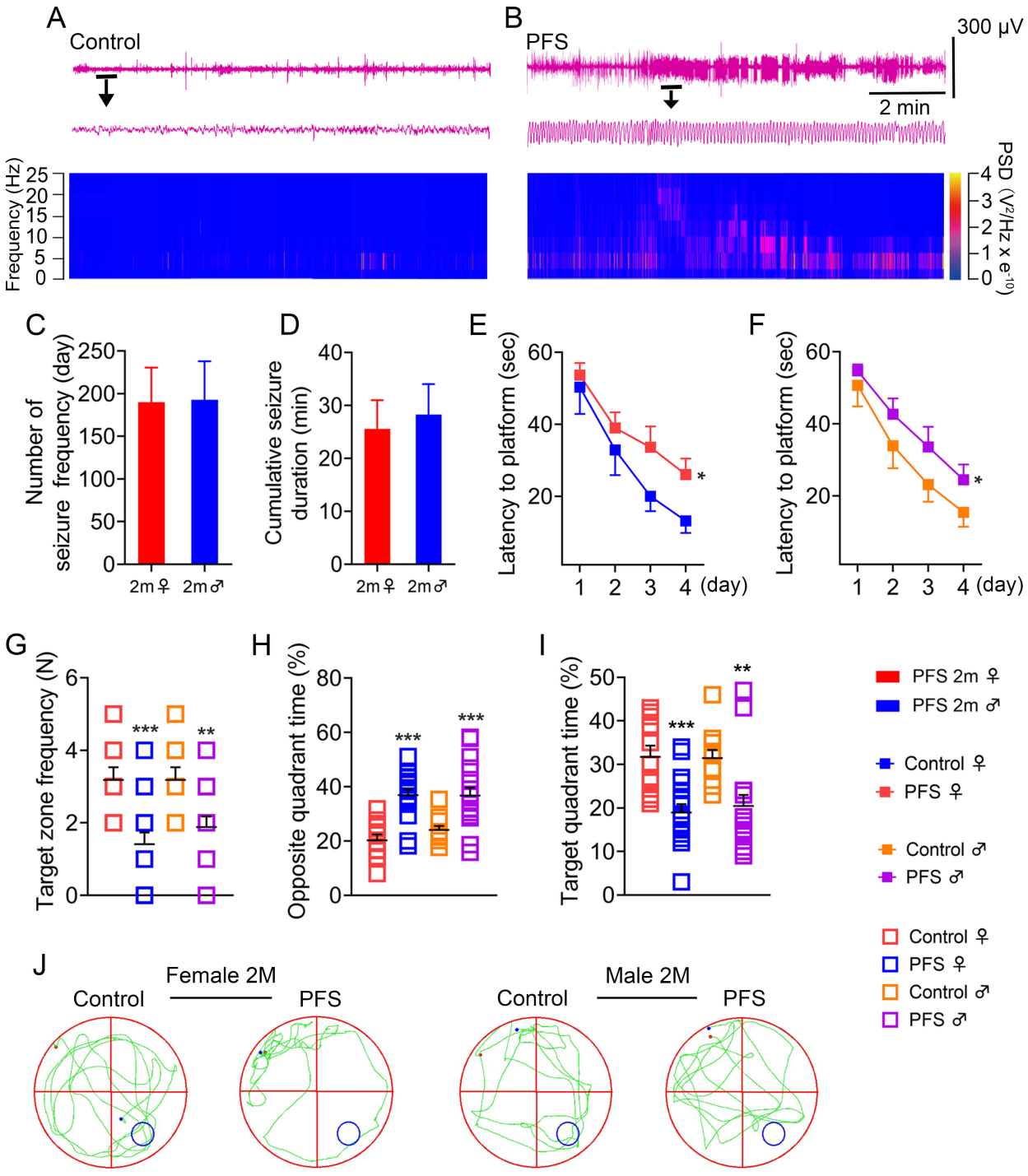

Fig. 2. Epileptic seizures and weakened learning and memory abilities after prolonged FS. (A,B) Representative EEGs and PSD analysis. (C) Average seizure frequency. (D) Cumulative seizure duration. (E,F) Latency to platform. (G) Target zone frequency. (H) Opposite quadrant time (%). (I) Target quadrant time (%). (J) Representative tracking. Control groups, female: n = 11, male: n = 11; PFS groups, female: n = 12, male: n = 12. *$p < 0.05$, **$p < 0.01$, ***$p < 0.001$, compared with control group. EEG, electroencephalography; PSD, power spectrum density; 2M, 2 months.

5H–J, the original Western blotting images are provided in the **Supplementary Material-WB**). FJB staining confirmed attenuated neuronal injury (e.g., DG, 24 h, $p < 0.001$; PC, 24 h, $p = 0.044$; Fig. 5K–M) in the AOA + prolonged FS group compared with the controls. These results indicated that AOA intervention attenuated succinate accumulation, mitophagy, and oxidative stress injury.

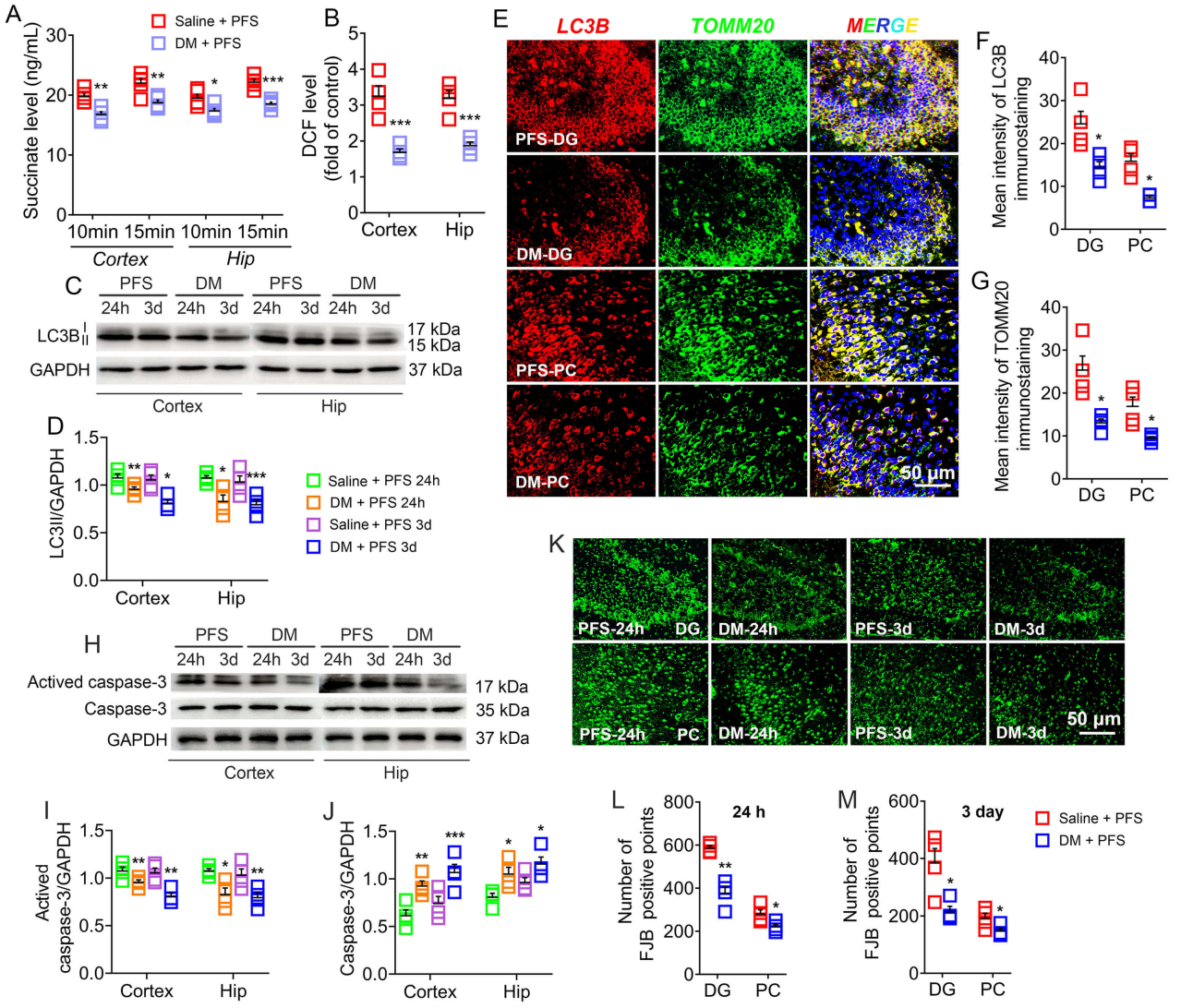

Fig. 3. DM treatment decreased succinate levels, mitophagy, oxidative stress injury. Decreased succinate (A) and DCF (B) levels in the hippocampus and cortex. (C,D) Decreased LC3B II levels evaluated by Western blotting. (E–G) Immunofluorescence results of TOMM20 (green) and LC3B (red). DAPI, blue. Gel bands (H) and quantification results (I,J) of caspase-3 and activated caspase-3. (K–M) FJB staining results. Succinate detection, n = 5/group; the others, n = 4/group. *$p < 0.05$, **$p < 0.01$, ***$p < 0.001$, compared with the controls. DM, dimethyl malonate. Scale bar = 50 μm.

3.6 AOA Treatment Reduced Seizure Severity and Defective Learning and Memory Ability in Prolonged FS-Treated Rats

EEG analysis indicated the decreased cumulative seizure number and duration in the AOA+ prolonged FS group (Fig. 6A,B). Water maze detection indicated that AOA intervention reversed the prolonged platform latency (Fig. 6C), with the elevation of the target quadrant time (Fig. 6D) and reduced opposite quadrant time (Fig. 6E). A representative trajectory is shown in Fig. 6F.

3.7 AICAR Treatment Reduced Succinate Levels, Mitophagy, Oxidative Stress Injury in Prolonged FS-Treated Rats

Similar to AOA, the treatment of AICAR, which is the specific inhibitor of PNC, led to decreased succinate (Fig. 7A) and DCF levels (Fig. 7B). LC3B II levels, detected by western blotting, were decreased in the hippocampus and cortex after AICAR treatment (Fig. 7C,D, the original Western blotting images are provided in the **Supplementary Material-WB**). Immunofluorescence confirmed a reduction in LC3B (Fig. 7E,F) and TOMM20 levels (Fig. 7E,G) after AICAR intervention. Compared with the saline + prolonged FS group, activated caspase-3 levels were significantly decreased, caspase-3 levels were increased (Fig.

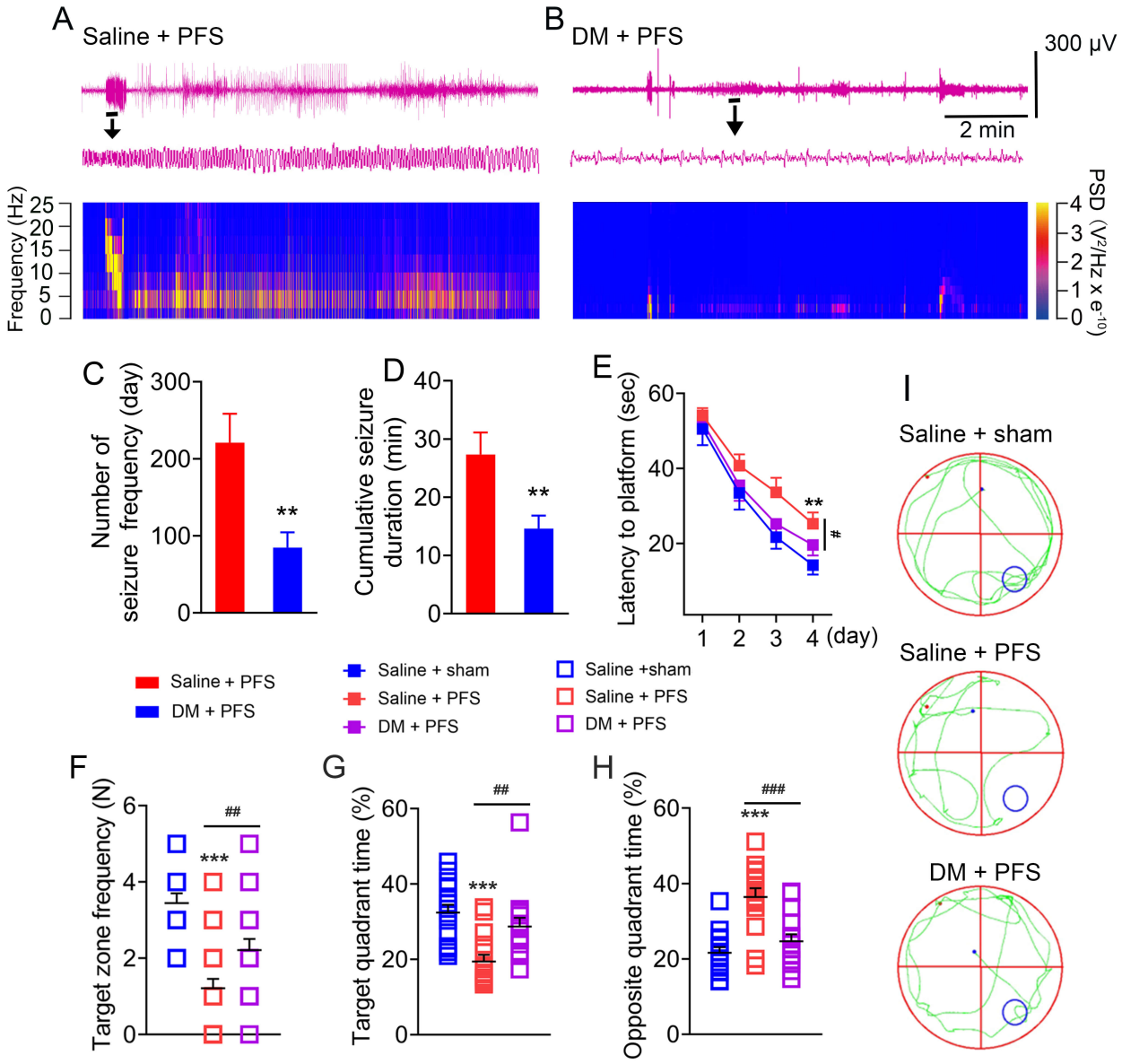

Fig. 4. DM treatment attenuated seizures and defective learning and memory abilities in prolonged FS-treated rats. (A,B) Representative EEGs and PSD analysis. (C) Average seizure frequency. (D) Cumulative seizure duration. (E) Latency to platform. (F) Target zone frequency. (G) Target quadrant time (%). (H) Opposite quadrant time (%). (I) Representative tracking. n = 12/group. $^{**}p < 0.01$, $^{***}p < 0.001$, compared with the controls, $^{\#}p < 0.05$, $^{\#\#}p < 0.01$, $^{\#\#\#}p < 0.001$, compared with each other.

7H–J, the original Western blotting images are provided in the **Supplementary Material-WB**). FJB results confirmed attenuated neuronal injury (Fig. 7K–M) in the AICAR + prolonged FS group.

3.8 AICAR Treatment Eased Seizure Severity and Defective Learning and Memory Ability in Prolonged FS-Treated Rats

EEG assessment indicated that AICAR treatment reduced the frequency and cumulative duration of seizures (Fig. 8A,B). Moreover, the water maze results verified that the latency to discover the platform in the AICAR + prolonged FS group was reduced (Fig. 8C), with elevated target quadrant duration (Fig. 8D) and decreased opposite quadrant duration (Fig. 8E). A representative trajectory is shown in Fig. 8F.

4. Discussion

Our study found that succinate levels increased significantly, accompanied by oxidative stress injury, seizures, and learning and memory defects, following prolonged FS. Treatment with the SDH inhibitor DM reduced succinate levels, accompanied by reduced levels of oxidative stress injury, attenuated seizures, and learning and mem-

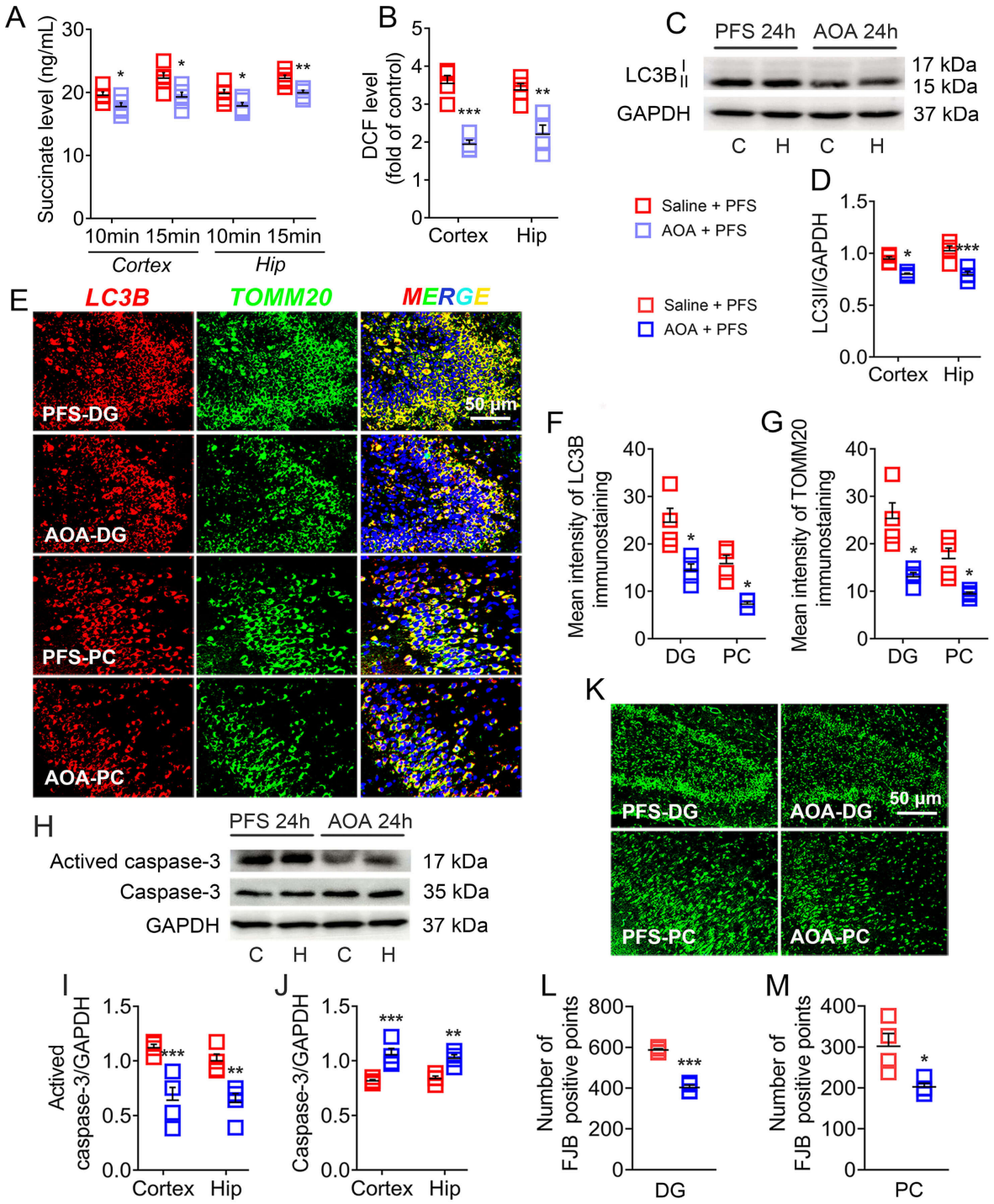

Fig. 5. AOA treatment decreased succinate levels, mitophagy, oxidative stress injury. Decreased succinate (A) and DCF (B) levels in the hippocampus and cortex. (C,D) Decreased LC3B II levels assessed by Western blotting. (E–G) Immunofluorescence results of TOMM20 (green) and LC3B (red). DAPI, blue. Gel bands (H) and quantification results (I,J) of caspase-3 and activated caspase-3. (K–M) FJB staining results in the DG and PC. Succinate detection, n = 5/group; the others, n = 4/group. *$p < 0.05$, **$p < 0.01$, ***$p < 0.001$, compared with the controls. AOA, aminooxyacetic acid. Scale bar = 50 μm.

ory deficits. Treatment with AICAR and AOA, inhibitors of PNC and MAS, respectively, played similar protective roles, accompanied by decreased succinate levels.

In this study, elevated succinate levels were observed after prolonged FS. As a butene diacid isomer, succinate has a structure similar to that of GABA and glutamate [32], and participates in the glutamate-GABA shunt and TCA cycle

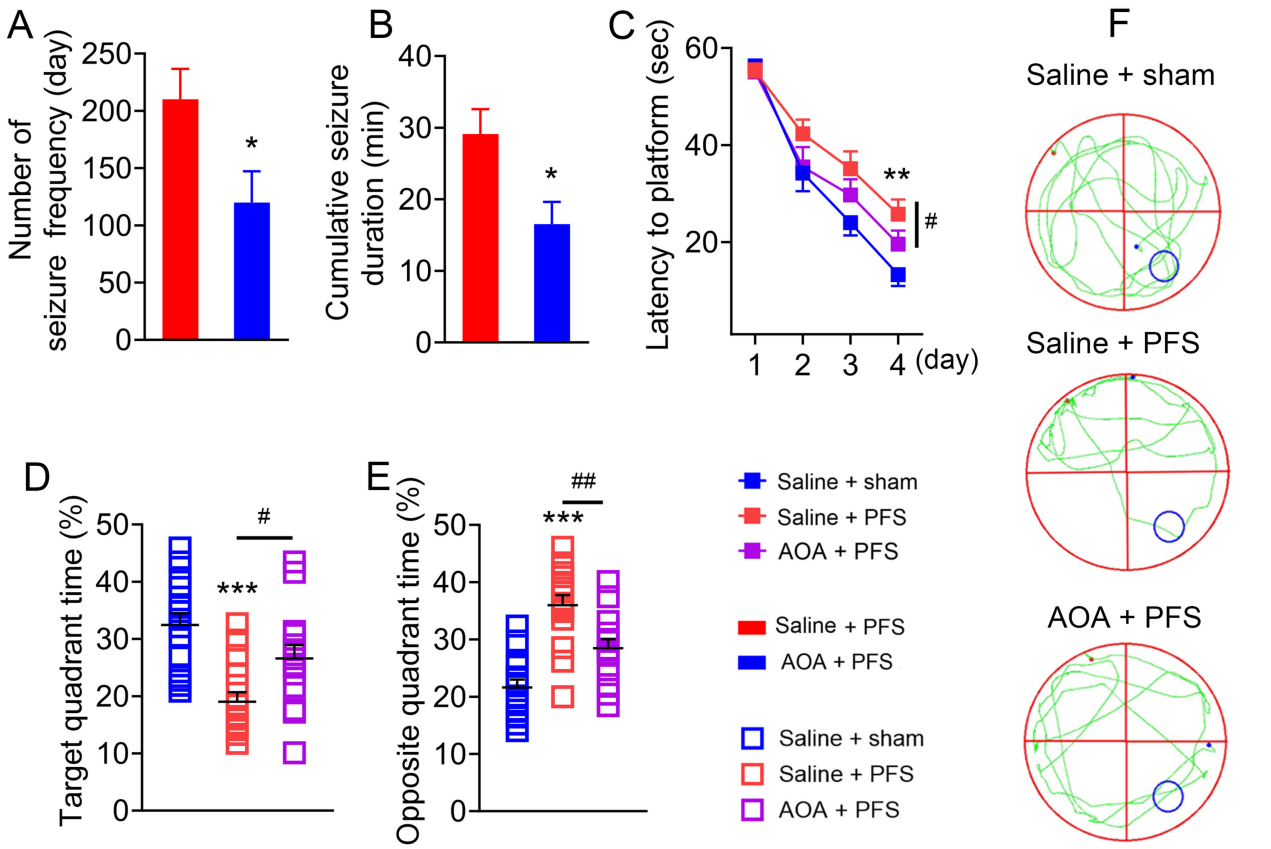

Fig. 6. AOA treatment reduced seizure severity and defective learning and memory ability in prolonged FS-treated rats. (A) Average seizure frequency. (B) Cumulative seizure duration. (C) Latency to platform. (D) Target quadrant time (%). (E) Opposite quadrant time (%). (F) Representative tracking. n = 12/group. $^{*}p < 0.05$, $^{**}p < 0.01$, $^{***}p < 0.001$, compared with the controls, $^{\#}p < 0.05$, $^{\#\#}p < 0.01$, compared with each other.

[33]. Succinate, GABA, and glutamate are mutually transformed via catalysis by specific enzymes [34]. Moreover, previous studies have confirmed that succinate may directly activate NMDA receptors and that succinate accumulation can trigger seizures through post-synaptic excitatory effects [8]. Succinate-triggered seizures are fully suppressed by treatment with MK-801, an NMDA receptor antagonist [8,35]. Moreover, our previous research verified that succinate accumulation promotes kainic acid-induced status epilepticus and that succinate treatment induces seizures in normal rats [12].

Hyperexcitability is an important pathological feature of both FS and epileptic seizures. Considering the excitatory actions of succinate and its accumulation following prolonged FS, we have reason to speculate that succinate accumulation contributes to prolonged FS-induced epileptogenesis and excitatory toxicity damage. Our experiments confirmed this hypothesis. Reducing succinate levels significantly attenuated epileptic seizures and neuronal damage.

Overexcitation can cause mitochondrial dysfunction [36]. Dysfunctional mitochondria produce more ROS, leading to oxidative stress, as well as increased cytoplasmic Ca^{2+} ($[Ca^{2+}]i$) concentration and glutamate release [37], which further induces excessive ROS production [38], aggravates oxidative stress-induced neuronal injury, and triggers seizures [38,39]. Consistent with the findings of previous studies, prolonged FS-induced seizures were along with significant oxidative stress injury in our study.

Succinate accumulation is closely related to ROS production. The oxidation of succinate provides a sufficiently high mitochondrial membrane potential for catabolism, resulting in the formation of excess ROS [40], leading to oxidative stress and neuronal injury [22]. These pathological changes are characteristic of epilepsy and play critical roles in epileptogenesis [41]. Therefore, succinate accumulation may promote the progression of FS to epilepsy via excess ROS production.

There are multiple electron transport chains to produce mitochondrial ROS, including complexes I-III [15]. Succinate drives reverse electron transport in complex I, which is critical for producing mitochondrial ROS [10,42]. SDH (complex II) is a succinate catalytic enzyme. Normally, succinate is oxidized to fumarate by SDH to main-

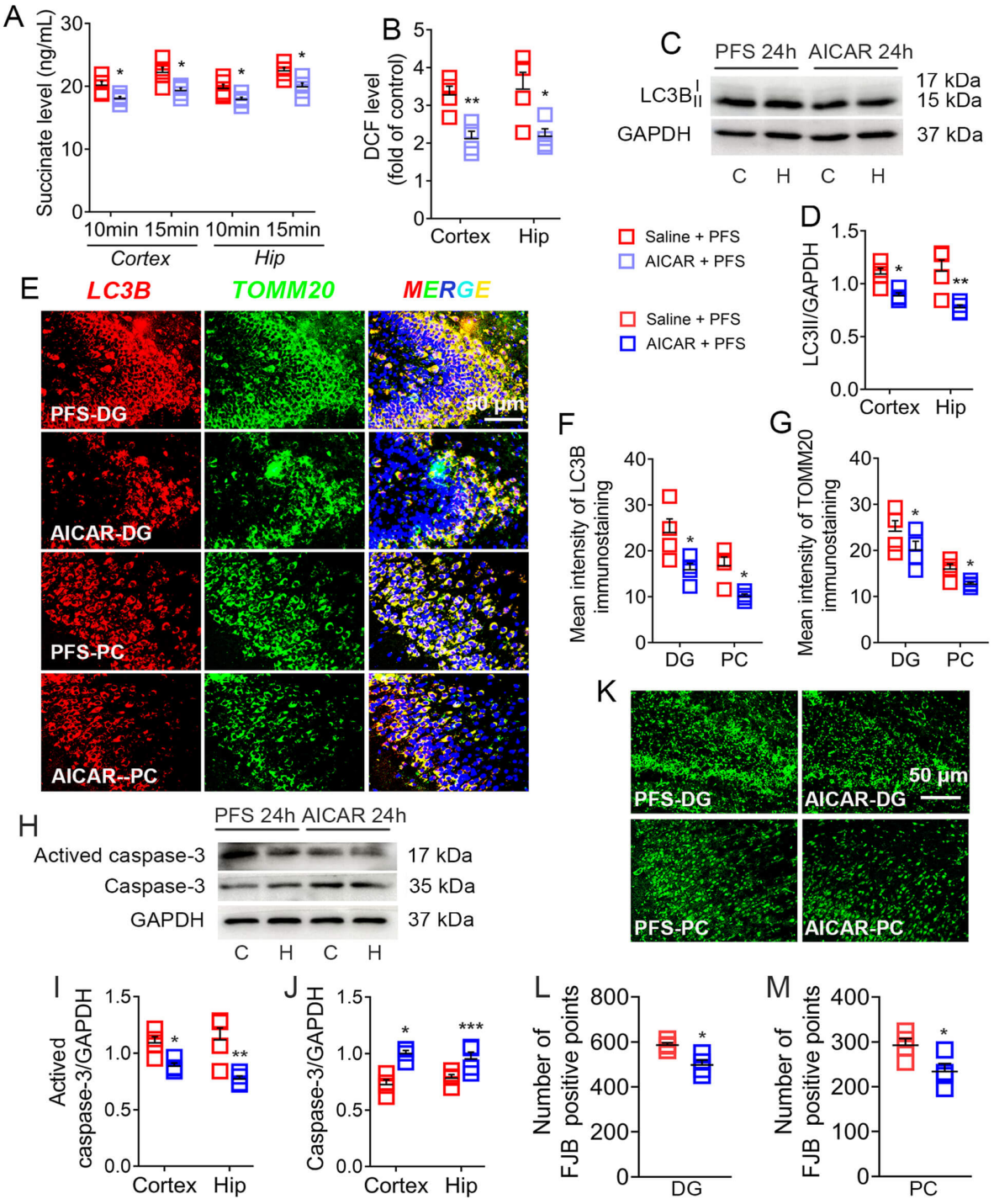

Fig. 7. AICAR treatment reduced succinate levels, mitophagy, oxidative stress injury in prolonged FS-treated rats. Decreased succinate (A) and DCF (B) levels in the hippocampus and cortex. (C,D) Decreased LC3B II levels assessed by Western blotting. (E–G) Immunofluorescence results of TOMM20 (green) and LC3B (red). DAPI, blue. Gel bands (H) and quantification results (I,J) of caspase-3 and activated caspase-3. (K–M) FJB staining results in the PC and DG. Succinate detection, n = 5/group; the others, n = 4/group. *$p < 0.05$, **$p < 0.01$, ***$p < 0.001$, compared with the controls. AICAR, 5-aminoimidazole-4-carboxamide-1-β-D-ribofuranoside. Scale bar = 50 μm.

tain mitochondrial ROS homeostasis [22]. However, in rats with ischemia-reperfusion injury, the reverse catalysis of SDH can cause succinate accumulation. Furthermore, accumulated succinate is re-oxidized and excess ROS is generated via reverse electron flow; decreasing succinate levels with SDH inhibitors leads to reduced mitochondrial

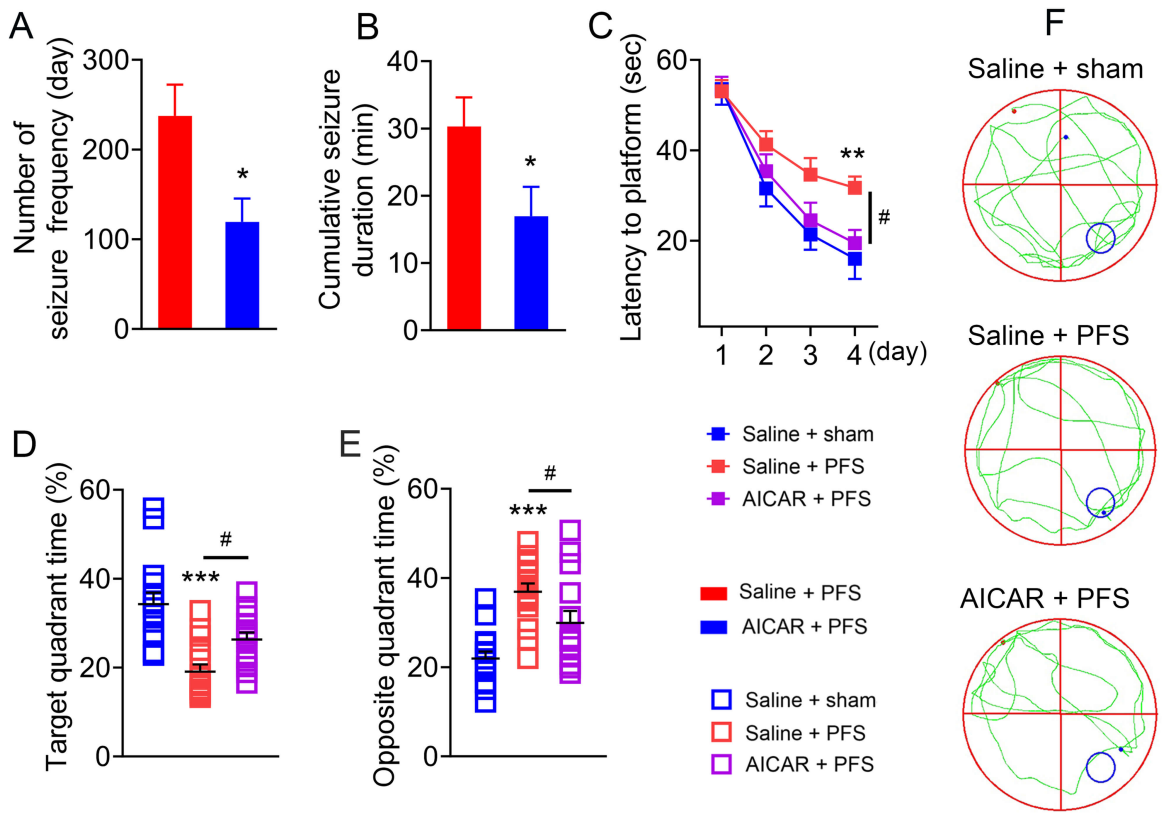

Fig. 8. AICAR treatment eased seizure severity and defective learning and memory ability in prolonged FS-treated rats. (A) Average seizure frequency. (B) Cumulative seizure duration. (C) Latency to platform. (D) Target quadrant time (%). (E) Opposite quadrant time (%). (F) Representative tracking. n = 12/group. $^{*}p < 0.05$, $^{**}p < 0.01$, $^{***}p < 0.001$, compared with the controls, $^{\#}p < 0.05$, compared with each other.

ROS production and attenuated oxidative stress-induced neuronal injury [10,23,42]. Consistent with previous reports, our study confirmed succinate accumulation following prolonged FS, with significantly increased mitochondrial ROS levels and neuronal damage [43]. Moreover, administration of DM, an SDH inhibitor, reduced succinate levels and attenuated oxidative stress injury. Our results suggest that the reversed catalysis of SDH may participate in succinate accumulation and that reducing succinate levels by inhibiting SDH may attenuate prolonged febrile seizures (PFS)-induced oxidative stress damage.

Interestingly, studies have confirmed that administration of SDH inhibitors leads to a considerable increase in succinate levels, with evoked seizures and neurotoxic effects [44,45]. It is reasonable to speculate that the different effects of the inhibitor may be determined by the functional status of SDH. In normal animals, SDH catalyzes succinate to fumarate, and treatment with its inhibitor induces succinate accumulation and neurotoxic effects [44,45]. However, in reverse catalysis of SDH, an inhibitor can reduce succinate levels and attenuate neurotoxicity.

Previous studies have identified possible sources of fumarate in the fumarate-succinate reverse catalysis pathway, including PNC and MAS, wherein fumarate is produced with a high $NADH/NAD^{+}$ ratio [46,47]. Subsequently, fumarate is reverse catalyzed by SDH, resulting in succinate accumulation [10]. In the present study, multiple inhibitors targeting PNC and MAS were administered to rats with prolonged FS. Similar to the role of SDH inhibitors, inhibition of the PNC or MAS pathway resulted in reduced succinate levels, accompanied by attenuated seizures and neuronal injury. Our results demonstrated a possible route for succinate accumulation during prolonged FS. This was mainly due to the reverse catalysis of SDH-targeting fumarate, which was supplemented by PNC and MAS.

5. Conclusions

FS has a high incidence in childhood and may have serious consequences including neuronal injury and epilepsy [1]. In clinical practice, approximately 13% of epilepsy patients have a history of FS [48]. Moreover, current antiseizure drugs may aggravate the neurological deficits induced by FS [6]. An unsatisfactory therapeutic status is closely related to unclear mechanisms of FS. Our results indicate that increased succinate levels promote prolonged

FS-induced oxidative stress injury and epileptogenesis and that reducing succinate accumulation may be a potential method for prolonged FS treatment. We also explored the underlying mechanisms and sources of succinate accumulation. Considering that succinate plays complex roles at the crossroads of several metabolic pathways [22], further research is expected to confirm the cell types of succinate accumulation, and elucidate the different biological functions in different neural cells, to enrich the cell-specific mechanism in FS-induced epileptogenesis.

Availability of Data and Materials

The data and material in this study are available from the corresponding authors on reasonable request.

Author Contributions

YY and XQW: study concept and design; drafting of the manuscript; YZ and HLS: study concept and design; technical and material support; YY, XQW, HZ, YRZ, XDW, SPY, BQZ, QYW, SL, HLS, and YZ: data acquisition and analysis. All authors contributed to editorial changes in the manuscript. All authors read and approved the final manuscript. All authors have participated sufficiently in the work and agreed to be accountable for all aspects of the work.

Ethics Approval and Consent to Participate

This work was approved by Shandong Medical and Pharmaceutical University Animal Experimentation Committee (No. 2022009), and in accordance with the National Institutes of Health Guide for the Care and Use of Laboratory Animals (no. 80-23, 1996 Revision) and ARRIVE 2.0.

Acknowledgment

The authors would like to thank Editage for English language editing.

Funding

This study was supported by the Natural Science Foundation of Shandong Province (ZR2021MH034, ZR2022MH059), National Natural Science Foundation of China (81573412), Key Research and Development Plan of Shandong Province (2018GSF121004).

Conflicts of Interest

The authors declare no conflicts of interest.

Supplementary Material

Supplementary material associated with this article can be found, in the online version, at https://doi.org/10.31083/JIN53240.

References

[1] Gould L, Delavale V, Plovnick C, Wisniewski T, Devinsky O. Are brief febrile seizures benign? A systematic review and narrative synthesis. Epilepsia. 2023; 64: 2539–2549. https://doi.org/10.1111/epi.17720

[2] Harris SA, George AG, Barrett KT, Scantlebury MH, Teskey GC. Febrile seizures lead to prolonged epileptiform activity and hyperoxia that when blocked prevents learning deficits. Epilepsia. 2022; 63: 2650–2663. https://doi.org/10.1111/epi.17371

[3] Suga T, Yoshida T, Yokoyama A, Hanami Y, Ashina K, Nakamura N, et al. Prolonged Febrile Seizure and Long-Term Neurological Sequelae in Otherwise Healthy Children. Annals of Neurology. 2025; 97: 688–693. https://doi.org/10.1002/ana.27192

[4] Lewis DV, Voyvodic J, Shinnar S, Chan S, Bello JA, Moshé SL, et al. Hippocampal sclerosis and temporal lobe epilepsy following febrile status epilepticus: The FEBSTAT study. Epilepsia. 2024; 65: 1568–1580. https://doi.org/10.1111/epi.17979

[5] Leitner DF, William C, Faustin A, Kanshin E, Snuderl M, McGuone D, et al. Raphe and ventrolateral medulla proteomics in sudden unexplained death in childhood with febrile seizure history. Acta Neuropathologica. 2024; 148: 76. https://doi.org/10.1007/s00401-024-02832-9

[6] Paul SP, Kirkham EN, Shirt B. Recognition and management of febrile convulsion in children. Nursing Standard. 2015; 29: 36–43. https://doi.org/10.7748/ns.29.52.36.e9927

[7] Moavero R, Santarone ME, Galasso C, Curatolo P. Cognitive and behavioral effects of new antiepileptic drugs in pediatric epilepsy. Brain & Development. 2017; 39: 464–469. https://doi.org/10.1016/j.braindev.2017.01.006

[8] Menéndez Méndez A, Smith J, Engel T. Neonatal Seizures and Purinergic Signalling. International Journal of Molecular Sciences. 2020; 21: 7832. https://doi.org/10.3390/ijms21217832

[9] Crespo M, León-Navarro DA, Martín M. Na^+/K^+- and Mg^{2+}-ATPases and Their Interaction with AMPA, NMDA and D_2 Dopamine Receptors in an Animal Model of Febrile Seizures. International Journal of Molecular Sciences. 2022; 23: 14638. https://doi.org/10.3390/ijms232314638

[10] Chouchani ET, Pell VR, Gaude E, Aksentijević D, Sundier SY, Robb EL, et al. Ischaemic accumulation of succinate controls reperfusion injury through mitochondrial ROS. Nature. 2014; 515: 431–435. https://doi.org/10.1038/nature13909

[11] Sinhorin VDG, Roehrs C, Pasin JSM, Bellé NAV, Rubin MA, Mello CF. Succinate causes oxidative damage through N-methyl-D-aspartate-mediated mechanisms. Brain Research. 2005; 1051: 66–71. https://doi.org/10.1016/j.brainres.2005.05.053

[12] Zhang Y, Zhang M, Zhu W, Yu J, Wang Q, Zhang J, et al. Succinate accumulation induces mitochondrial reactive oxygen species generation and promotes status epilepticus in the kainic acid rat model. Redox Biology. 2020; 28: 101365. https://doi.org/10.1016/j.redox.2019.101365

[13] Scalise S, Zannino C, Lucchino V, Lo Conte M, Abbonante V, Benedetto GL, et al. Ascorbic acid mitigates the impact of oxidative stress in a human model of febrile seizure and mesial temporal lobe epilepsy. Scientific Reports. 2024; 14: 5941. https://doi.org/10.1038/s41598-024-56680-4

[14] Cheng Y, Zhai Y, Yuan Y, Li H, Zhao W, Fan Z, et al. Xenon inhalation attenuates neuronal injury and prevents epilepsy in febrile seizure Sprague-Dawley pups. Frontiers in Cellular Neuroscience. 2023; 17: 1155303. https://doi.org/10.3389/fncel.2023.1155303

[15] Chandel NS, McClintock DS, Feliciano CE, Wood TM, Melendez JA, Rodriguez AM, et al. Reactive oxygen species generated at mitochondrial complex III stabilize hypoxia-inducible factor-1α during hypoxia: a mechanism of O2 sensing. The Journal of Biological Chemistry. 2000; 275: 25130–25138. https://doi.org/10.1074/jbc.M001914200

[16] Wu WL, Gong XX, Qin ZH, Wang Y. Molecular mechanisms of excitotoxicity and their relevance to the pathogenesis of neurodegenerative diseases-an update. Acta Pharmacologica Sinica. 2025; 46: 3129–3142. https://doi.org/10.1038/s41401-025-01576-w

[17] Xu X, Pang Y, Fan X. Mitochondria in oxidative stress, inflammation and aging: from mechanisms to therapeutic advances. Signal Transduction and Targeted Therapy. 2025; 10: 190. https://doi.org/10.1038/s41392-025-02253-4

[18] Xing J, Han D, Xu D, Li X, Sun L. CREB Protects against Temporal Lobe Epilepsy Associated with Cognitive Impairment by Controlling Oxidative Neuronal Damage. Neurodegenerative Diseases. 2019; 19: 225–237. https://doi.org/10.1159/000507023

[19] Beckstead MJ, Howell RD. Progressive parkinsonism due to mitochondrial impairment: Lessons from the MitoPark mouse model. Experimental Neurology. 2021; 341: 113707. https://doi.org/10.1016/j.expneurol.2021.113707

[20] Oh CJ, Kim MJ, Lee JM, Kim DH, Kim IY, Park S, et al. Inhibition of pyruvate dehydrogenase kinase 4 ameliorates kidney ischemia-reperfusion injury by reducing succinate accumulation during ischemia and preserving mitochondrial function during reperfusion. Kidney International. 2023; 104: 724–739. https://doi.org/10.1016/j.kint.2023.06.022

[21] Tabata Fukushima C, Dancil IS, Clary H, Shah N, Nadtochiy SM, Brookes PS. Reactive oxygen species generation by reverse electron transfer at mitochondrial complex I under simulated early reperfusion conditions. Redox Biology. 2024; 70: 103047. https://doi.org/10.1016/j.redox.2024.103047

[22] Tretter L, Patocs A, Chinopoulos C. Succinate, an intermediate in metabolism, signal transduction, ROS, hypoxia, and tumorigenesis. Biochimica et Biophysica Acta. 2016; 1857: 1086–1101. https://doi.org/10.1016/j.bbabio.2016.03.012

[23] Andrienko TN, Pasdois P, Pereira GC, Ovens MJ, Halestrap AP. The role of succinate and ROS in reperfusion injury - A critical appraisal. Journal of Molecular and Cellular Cardiology. 2017; 110: 1–14. https://doi.org/10.1016/j.yjmcc.2017.06.016

[24] Mills EL, Kelly B, Logan A, Costa ASH, Varma M, Bryant CE, et al. Succinate Dehydrogenase Supports Metabolic Repurposing of Mitochondria to Drive Inflammatory Macrophages. Cell. 2016; 167: 457–470.e13. https://doi.org/10.1016/j.cell.2016.08.064

[25] Chen B, Feng B, Tang Y, You Y, Wang Y, Hou W, et al. Blocking GluN2B subunits reverses the enhanced seizure susceptibility after prolonged febrile seizures with a wide therapeutic time-window. Experimental Neurology. 2016; 283: 29–38. https://doi.org/10.1016/j.expneurol.2016.05.034

[26] Wu D, Feng B, Dai Y, Wu X, Chen B, Xu C, et al. Intergenerational Transmission of Enhanced Seizure Susceptibility after Febrile Seizures. EBioMedicine. 2017; 17: 206–215. https://doi.org/10.1016/j.ebiom.2017.02.006

[27] Zhang M, Cheng Y, Zhai Y, Cui Y, Zhang W, Sun H, et al. Attenuated succinate accumulation relieves neuronal injury induced by hypoxia in neonatal mice. Cell Death Discovery. 2022; 8: 138. https://doi.org/10.1038/s41420-022-00940-7

[28] Zhang M, Cheng Y, Zhai Y, Yuan Y, Hu H, Meng X, et al. Attenuated iron stress and oxidative stress may participate in anti-seizure and neuroprotective roles of xenon in pentylenetetrazole-induced epileptogenesis. Frontiers in Cellular Neuroscience. 2022; 16: 1007458. https://doi.org/10.3389/fncel.2022.1007458

[29] Zhang H, Jiao W, Cui H, Sun Q, Fan H. Combined exposure of alumina nanoparticles and chronic stress exacerbates hippocampal neuronal ferroptosis via activating IFN-γ/ASK1/JNK signaling pathway in rats. Journal of Hazardous Materials. 2021; 411: 125179. https://doi.org/10.1016/j.jhazmat.2021.125179

[30] Yu LM, Zhang WH, Han XX, Li YY, Lu Y, Pan J, et al. Hypoxia-Induced ROS Contribute to Myoblast Pyroptosis during Obstructive Sleep Apnea via the NF-κB/HIF-1α Signaling Pathway. Oxidative Medicine and Cellular Longevity. 2019; 2019: 4596368. https://doi.org/10.1155/2019/4596368

[31] He G, Nie JJ, Liu X, Ding Z, Luo P, Liu Y, et al. Zinc oxide nanoparticles inhibit osteosarcoma metastasis by downregulating β-catenin via HIF-1α/BNIP3/LC3B-mediated mitophagy pathway. Bioactive Materials. 2022; 19: 690–702. https://doi.org/10.1016/j.bioactmat.2022.05.006

[32] Treiman DM. GABAergic mechanisms in epilepsy. Epilepsia. 2001; 42: 8–12. https://doi.org/10.1046/j.1528-1157.2001.042suppl.3008.x

[33] Balázs R, Machiyama Y, Hammond BJ, Julian T, Richter D. The operation of the gamma-aminobutyrate bypath of the tricarboxylic acid cycle in brain tissue in vitro. The Biochemical Journal. 1970; 116: 445–461. https://doi.org/10.1042/bj1160445

[34] Bouché N, Fait A, Bouchez D, Møller SG, Fromm H. Mitochondrial succinic-semialdehyde dehydrogenase of the gamma-aminobutyrate shunt is required to restrict levels of reactive oxygen intermediates in plants. Proceedings of the National Academy of Sciences of the United States of America. 2003; 100: 6843–6848. https://doi.org/10.1073/pnas.1037532100

[35] Zeevalk GD, Derr-Yellin E, Nicklas WJ. Relative vulnerability of dopamine and GABA neurons in mesencephalic culture to inhibition of succinate dehydrogenase by malonate and 3-nitropropionic acid and protection by NMDA receptor blockade. The Journal of Pharmacology and Experimental Therapeutics. 1995; 275: 1124–1130.

[36] Perone I, Ghena N, Wang J, Mackey C, Wan R, Malla S, et al. Mitochondrial SIRT3 Deficiency Results in Neuronal Network Hyperexcitability, Accelerates Age-Related Aβ Pathology, and Renders Neurons Vulnerable to Aβ Toxicity. Neuromolecular Medicine. 2023; 25: 27–39. https://doi.org/10.1007/s12017-022-08713-2

[37] Del Arroyo AG, Hadjihambi A, Sanchez J, Turovsky E, Kasymov V, Cain D, et al. NMDA receptor modulation of glutamate release in activated neutrophils. EBioMedicine. 2019; 47: 457–469. https://doi.org/10.1016/j.ebiom.2019.08.004

[38] Doser RL, Knight KM, Deihl EW, Hoerndli FJ. Activity-dependent mitochondrial ROS signaling regulates recruitment of glutamate receptors to synapses. elife. 2024; 13: e92376. https://doi.org/10.7554/eLife.92376

[39] Parsons ALM, Bucknor EMV, Castroflorio E, Soares TR, Oliver PL, Rial D. The Interconnected Mechanisms of Oxidative Stress and Neuroinflammation in Epilepsy. Antioxidants. 2022; 11: 157. https://doi.org/10.3390/antiox11010157

[40] Korshunov SS, Skulachev VP, Starkov AA. High protonic potential actuates a mechanism of production of reactive oxygen species in mitochondria. FEBS Letters. 1997; 416: 15–18. https://doi.org/10.1016/s0014-5793(97)01159-9

[41] Moos WH, Faller DV, Glavas IP, Kanara I, Kodukula K, Pernokas J, et al. Epilepsy: Mitochondrial connections to the 'Sacred' disease. Mitochondrion. 2023; 72: 84–101. https://doi.org/10.1016/j.mito.2023.08.002

[42] Valdez LB, Zaobornyj T, Bandez MJ, López-Cepero JM, Boveris A, Navarro A. Complex I syndrome in striatum and frontal cortex in a rat model of Parkinson disease. Free Radical Biology & Medicine. 2019; 135: 274–282. https://doi.org/10.1016/j.freeradbiomed.2019.03.001

[43] Chen B, Xu C, Wang Y, Lin W, Wang Y, Chen L, et al. A disinhibitory nigra-parafascicular pathway amplifies seizure in temporal lobe epilepsy. Nature Communications. 2020; 11: 923. https://doi.org/10.1038/s41467-020-14648-8

[44] Hassel B, Sonnewald U. Selective inhibition of the tricarboxylic acid cycle of GABAergic neurons with 3-nitropropionic acid in vivo. Journal of Neurochemistry. 1995; 65: 1184–1191. https:

//doi.org/10.1046/j.1471-4159.1995.65031184.x
[45] Urbanska EM, Blaszczak P, Saran T, Kleinrok Z, Turski WA. Mitochondrial toxin 3-nitropropionic acid evokes seizures in mice. European Journal of Pharmacology. 1998; 359: 55–58. https://doi.org/10.1016/s0014-2999(98)00648-7
[46] Easlon E, Tsang F, Skinner C, Wang C, Lin SJ. The malate-aspartate NADH shuttle components are novel metabolic longevity regulators required for calorie restriction-mediated life span extension in yeast. Genes & Development. 2008; 22: 931–944. https://doi.org/10.1101/gad.1648308
[47] Sridharan V, Guichard J, Li CY, Muise-Helmericks R, Beeson CC, Wright GL. O(2)-sensing signal cascade: clamping of O(2) respiration, reduced ATP utilization, and inducible fumarate respiration. American Journal of Physiology. Cell Physiology. 2008; 295: C29–C37. https://doi.org/10.1152/ajpcell.00466.2007
[48] Moreno de Flagge N. Crisis febriles simples y complejas, epilepsia generalizada con crisis febriles plus, FIRES y nuevos síndromes [Simple febrile seizure, complex seizure, generalized epilepsy with febrile seizure plus, FIRES and new syndromes]. Medicina. 2013; 73: 63–70. (In Spanish)